

# Probing Lorentz Invariance Violation at High-Energy Colliders via Intermediate Massive Boson Mass Measurements: Z Boson Example

Z. Kepuladze<sup>1</sup>, J. Jejelava<sup>1</sup>

<sup>1</sup>Andronikashvili Institute of Physics, Tbilisi State University, Ilia State University

## Abstract

Lorentz invariance (LI) is a foundational principle of modern physics, yet its possible violation (LIV) remains an intriguing window to physics beyond the Standard Model. While stringent constraints exist in the electromagnetic and hadronic sectors, the weak sector—particularly unstable bosons—remains largely unexplored. In this work, based on our recent studies and conference presentation, we analyze how LIV manifests in high-energy collider experiments, focusing on modifications of Z boson dispersion relations and their impact on resonance measurements in Drell–Yan processes. We argue that precision measurements of resonance masses at colliders provide sensitivity to LIV at the level of  $10^{-9}$ , comparable to bounds derived from cosmic rays. We also discuss the interplay between LIV and gauge invariance, highlighting why only specific operators provide physical effects. The phenomenological implications for both Z and W bosons are outlined, with emphasis on experimental strategies for current and future colliders.

## 1 Introduction

Lorentz invariance (LI) underpins the structure of quantum field theory and general relativity. Yet possible violations of this symmetry are theoretically motivated. Spontaneous Lorentz symmetry breaking can give rise to emergent vector or tensor degrees of freedom, which may act as Goldstone modes of spacetime symmetry violation [1]. Alternatively, LIV can appear as a mechanism for ultraviolet completion, rendering theories finite, as in Hořava’s construction [2]. At low energies, if present, LIV should be strongly suppressed, but in the ultra–high-energy domain it may have significant phenomenological consequences.

The motivation for studying LIV partly comes from cosmic ray physics. The famous Greisen–Zatsepin–Kuzmin (GZK) cutoff [3] predicts that ultra–high-energy cosmic rays above  $\sim 5 \times 10^{19}$  eV should be strongly attenuated by interactions with the cosmic microwave background. However, experiments such as AGASA and, later, the Pierre Auger Observatory reported excess events beyond the GZK bound, sparking interest in LIV as a possible explanation [4,5]. Such cosmic ray observations thus continue to provide motivation for precise LIV studies.

Another motivation comes from neutrino physics. The possibility of neutrinos traveling at speeds slightly different from light has been considered in multiple contexts. Early hints, such as the controversial OPERA result, suggested superluminal neutrinos, though

this was later shown to be an experimental error. Nonetheless, neutrino time-of-flight experiments and supernova neutrino observations (e.g., SN1987A) constrain deviations from the speed of light at the level of  $10^{-9}$  or better [6]. These are directly relevant because they probe LIV in the weak sector, where constraints remain far weaker than in the electromagnetic one.

Thus, cosmic ray and neutrino data both highlight the importance of searching for LIV in controlled environments such as high-energy colliders. While astrophysical observations give very stringent limits in some channels, colliders allow systematic and model-independent tests, especially for unstable weak bosons that cannot be probed astrophysically.

## 2 Constraints and Open Windows

The tightest constraints on LIV arise mostly from astrophysical processes, since cosmic rays may carry energies far beyond those accessible at accelerators or other Earth-based experiments. If we describe these restrictions in the language of possible deviations from the maximal attainable velocity for a given particle species (a particle’s “speed of light,” so to speak) [7], defined as  $\delta = \Delta c/c$ , then the following constraints can be quoted. For electrons:  $|\delta_e| < 10^{-19}$  [8, 9],  $|\delta_e - \delta_\gamma| < 5 \cdot 10^{-19}$  [10]. Restrictions on photons and protons fall in approximately the same range [8]. These arise from the non-observation of otherwise expected effects in the presence of LIV, such as photon decay and vacuum Cherenkov radiation (generally derived from threshold-energy arguments), tests of rotating optical cavities, vacuum birefringence, dispersion, Michelson–Morley–type resonators, or time-of-flight measurements. Bounds from these processes are so strong that they effectively rule out LIV in the QED sector at accessible scales.

Neutrinos provide a different picture. Time-of-flight measurements constrain their velocity relative to light. Supernova SN1987A neutrino arrival times imply  $|\delta_\nu| < 10^{-9}$  at energies of tens of MeV. At higher energies, IceCube measurements of PeV neutrinos place bounds at the level of  $10^{-10}$ – $10^{-11}$ . Atmospheric neutrino oscillations observed by Super-Kamiokande constrain certain LIV coefficients to  $10^{-8}$  in the GeV range.

In general, unstable particles—among them the weak bosons W and Z, which are both unstable and short-lived—evade such astrophysical probes. Their dispersion relations have never been directly tested outside collider environments. Consequently, the weak sector remains essentially unconstrained with respect to LIV. Whether this is a special feature of the weak sector remains to be determined. At the same time, this gap represents an open experimental window: accelerator experiments can probe parameter space that astrophysical methods cannot access. Collider studies of massive intermediate boson resonances therefore allow us to test LIV systematically in a sector that has remained hidden from astrophysical scrutiny.

The present contribution builds upon our recent studies [11, 12].

## 3 Testing LIV at Accelerators: Concept

Whatever the origin of LIV might be, the low-energy phenomenology can always be parameterized by possible modifications to particle propagation and interactions. If the preferred direction of LIV is fixed in spacetime by a timelike or spacelike unit vector

$n_\mu = (n_0, \vec{n})$ <sup>1</sup>, one of the simplest renormalizable interactions between the vector field  $A_\mu$  and fermion field  $\Psi$  may take the form

$$e\delta_{\text{int}}(A_\mu n^\mu)\bar{\Psi}(\gamma_\nu n^\nu)\Psi \quad (1)$$

To detect such modifications at accelerators, one usually examines their effect on cross sections, which acquire the general form

$$\sigma_{LIV} = \sigma_{LI}(1 + \delta_{\text{int}}f(\Omega, n)) \quad (2)$$

where  $f(\Omega, n)$  encodes the interplay between the preferred LIV direction  $n_\mu$  and the orientation of the process in spacetime. Because  $n_\mu$  picks out a special direction, it introduces anisotropy into the process. Since an accelerator rotates with the Earth, the relative orientation with respect to  $n_\mu$  also changes with sidereal time. Therefore, daily modulations should emerge in the cross section if LIV is present and the experimental accuracy is sufficient.

Searches for such modulations have been conducted at the Large Hadron Collider (LHC), yielding limits of  $|\delta_{\text{int}}| < 10^{-5}$  [13, 14]. While the specific modifications studied in those analyses originated in the quark sector, their functional form is quite general and can be applied to a broad class of LIV operators, including the interaction above. Provided that  $f(\Omega, n)$  has no strong energy dependence, these bounds can be generalized accordingly.

A noticeable property of this form of  $\sigma_{LIV}$  is that LIV contributions always enter at the same order in  $\delta_{\text{int}}$ . Detectability therefore depends only on experimental precision, essentially independent of the energy scale. This situation contrasts with modifications of the dispersion relation, which in their simplest form can be written as

$$p^\mu p_\mu = M_{B,\text{eff}}^2 = M_B^2 + \delta E^2 \quad (3)$$

Here  $p_\mu = (E, \vec{p})$  is the four-momentum and  $M_B$  the given boson mass. We have also introduced notion of the effective mass. In this case the LIV term competes with the mass term, and the hierarchy between them changes with energy, making LIV effects increasingly accessible at high energies. Scattering processes mediated by a massive intermediate boson therefore become highly sensitive to such modifications in the resonance region.

For the boson with (3), one can approximate [15]

$$\Gamma_{LIV} = \frac{M_{B,\text{eff}}^2}{M_B^2} \Gamma_{LI} \quad (4)$$

so the unstable boson propagator becomes

$$\begin{aligned} D &= \frac{i}{p_\alpha^2 - M_B^2} \rightarrow \frac{i}{p_\alpha^2 - (M_{B,\text{eff}} - ip_0\Gamma_{LIV}/2M_{B,\text{eff}})^2} \\ &= \frac{i}{p_\alpha^2 - M_{B,\text{eff}}^2(1 - i\Gamma_{LI}/2M_B)^2} \end{aligned} \quad (5)$$

---

<sup>1</sup>The preferred direction, fixed by the  $n_\mu$  vector, transforms as a constant four-vector under Lorentz transformations. The explicit form written in the text corresponds to a particular reference frame; in other frames the components of  $n_\mu$  change accordingly, while its invariant character as a preferred direction remains.

Consequently, the cross section is

$$\sigma_B^{LIV} \sim |D_B|^2 \quad (6)$$

and the resonance mass  $M_{res}$  now measures the effective mass instead:

$$M_{res}^2 = M_{B,eff}^2 (1 - \Gamma_{LIV}^2 / 4M_B^2) \quad (7)$$

Applying this framework to the weak  $Z$  boson, and comparing the resonance mass shift with the current precision of  $M_Z$ , one finds that at LHC energies of  $E = 14$  TeV, the present experimental uncertainty of  $\Delta M_Z = |M_Z - M_{Zresonance}| \approx 2$  MeV [16] implies

$$|\delta| \approx \frac{2M_Z \Delta M_Z}{E^2} \approx 2 \cdot 10^{-9} \quad (8)$$

This level of sensitivity is comparable to astrophysical constraints for the neutrinos.

Such a preliminary result is already convincing enough to justify further investigation. In the next section we turn to the realistic Drell–Yan cross section mediated by the neutral weak boson. When considering Lorentz invariance violation in the weak sector, the  $Z$  boson provides the cleanest probe due to its narrow resonance and well-measured leptonic decay modes.

## 4 Modified Dynamics of the $Z$ Boson

To introduce modified dynamics for the neutral weak boson, a natural starting point is to modify the kinetic term of the  $Z$ -boson Lagrangian. For a preferred direction fixed in spacetime by the vector  $n_\mu$ , the kinetic term that introduces LIV, modifies the dispersion relation, and is constrained by two derivatives (i.e. is renormalizable), is

$$\Delta L_{LIV} = \frac{\delta_{LIV}}{2} (\partial_n Z^\mu) (\partial_n Z_\mu), \quad \partial_n \equiv n_\mu \partial^\mu \quad (9)$$

Alongside this term, one can introduce additional LIV operators,

$$\Delta L_{LIV} = \frac{\delta_{LIV}}{2} (\partial_n Z^\mu) (\partial_n Z_\mu) + \frac{\delta_{1LIV}}{2} (\partial_\mu Z_n) (\partial^\mu Z_n) + \delta_{2LIV} (\partial_\mu Z^\mu) (\partial_n Z_n) \quad (10)$$

with  $Z_n \equiv n_\mu Z^\mu$ .

These operators are often introduced because in the literature there is a frequent attempt to enforce a gauge-invariant (GI) form. In that case one sets  $\delta_{LIV} = \delta_{1LIV} = -\delta_{2LIV}$ . However, neither of the two additional terms influences the dispersion relation. More importantly, LIV and GI do not go hand in hand. One can safely claim that if we want physical LIV in a theory, gauge invariance must be broken at least slightly. In fact, it is possible to obtain GI precisely from the demand that LIV be physically unobservable [1, 17].

A simple demonstration is as follows. If we introduce a mass term  $m^2 (n_\mu A^\mu)^2$  (or any operator for that matter of the form  $F(n_\mu A^\mu)$ ,  $F(n_\mu A^\mu) \bar{\Psi} \Psi$ ,  $F(n_\mu A^\mu) \bar{\Psi} n_\lambda \gamma^\lambda \Psi$ , etc.) into an otherwise GI theory, then by performing a gauge transformation toward the axial gauge  $n_\mu A^\mu = 0$  we can effectively eliminate LIV from the theory. Instead of genuine LIV, we only succeed in fixing a particular gauge. The same is true for any  $F(A^\mu)$ . If the

gauge equation  $F(A^\mu + \partial^\mu \omega) = 0$  has a solution for  $\omega$  for arbitrary  $A^\mu$ , then  $F(A^\mu) = 0$  will become simply a gauge choice. If this gauge equation does not have a solution, gauge invariance is broken and physical LIV necessarily manifests.

A distinct case arises if  $F(A^\mu)$  has a manifestly GI form itself, for example  $F(A^\mu) \sim \delta n_\mu F^{\mu\lambda} n^\nu F_{\nu\lambda}$ , where  $F_{\nu\lambda} = \partial_\nu A_\lambda - \partial_\lambda A_\nu$  and  $\delta$  is the LIV strength. In such a scenario, GI remains exact and gauge can be fixed by our convenience. At first glance everything appears consistent: the massless vector field still describes two propagating degrees of freedom and the Coulomb law is intact. But once  $U(1)$  symmetry is broken, a problem emerges: the vector field still carries only two degrees of freedom instead of behaving as a massive vector should. In other words, the theory becomes inconsistent with reality.

Even manifestly GI LIV fermion operators of “mass” type, such as  $\bar{\Psi} n_\lambda \gamma^\lambda \Psi$  or  $\bar{\Psi} n_\lambda \gamma^\lambda \gamma^5 \Psi$ , share this issue. The first can be gauged away by a corresponding transformation, while the second explicitly breaks GI. This may seem counter-intuitive, but the problem becomes evident if we calculate the vector-field polarization loop diagram, since this axial mass term is used for radiative generation of Chern-Simons term. For example, with  $S(k) = 1/(k - b\gamma^5)$ , one finds

$$p_\mu \Pi^{\mu\nu}(p; b) = p_\mu \int \frac{d^4 q}{(2\pi)^4} \text{Tr}[\gamma^\mu S(q) \gamma^\nu S(q - p)] \neq 0 \quad (11)$$

which explicitly signals a violation of GI [11]. In principle, an easier way to check gauge invariance is by examining the modified Compton scattering matrix element. It is straightforward to see that if the matrix element takes the form  $\xi_{1\mu}(k_1) \xi_{2\nu}(k_2) \mathcal{M}^{\mu\nu}$ , where  $\xi_{1\mu}(k_1)$  and  $\xi_{2\nu}(k_2)$  are the photon polarization vectors, then the gauge invariance condition  $k_{1\mu} \mathcal{M}^{\mu\nu} = 0$  is not satisfied—even at linear order in  $b^\nu$ .

In short, we are demotivated from using GI setups for LIV operators. The scheme outlined above justifies focusing on corrections that affect the dispersion relation directly. Moreover, once LIV operators are introduced, the gauge choice must also be specified, since even a small breaking of GI renders different gauges inequivalent. For concreteness, in what follows we proceed with (9) and assume the Standard Model (SM) in the unitary gauge. While it is interesting to speculate about the form of a LIV setup in the unbroken electroweak phase that could lead here, for our purposes this is not essential.

With (9) the dispersion relation of the Z boson is modified as

$$Q_\mu Q^\mu = M_{eff}^2 = M_Z^2 + \delta_{LIV} Q_n^2 \quad (12)$$

where  $Q_\mu$  is the four-momentum of the particle,  $Q_n \equiv n_\mu Q^\mu$  and  $M_Z$  is the Z boson mass. Here we reintroduce the notion of an effective mass.

The corresponding decay width can be written as [12]

$$\Gamma_{eff}(Q) \approx \frac{M_{eff}^2}{M_Z^2} \Gamma_{SM}(Q) = \frac{M_{eff}^2}{Q_0 M_Z} \Gamma_{0SM} \quad (13)$$

where  $\Gamma_{SM}$  is SM expression and  $\Gamma_{0SM}$  is its rest frame form.

For the propagator we obtain an expression resembling the massive vector propagator in unitary gauge:

$$\frac{-i}{Q_\lambda^2 - M_{eff}^2} \left( g_{\mu\nu} - \frac{Q_\mu Q_\nu}{M_{eff}^2} \right) \quad (14)$$

Usually, unstable massive field propagators are corrected by loop contributions, which acquire an imaginary part near the pole. By the optical theorem this imaginary contribution is proportional to the decay rate of the intermediate particle. Implementing this yields the replacement

$$M_{eff} \rightarrow M_{eff} - iQ_0\Gamma_{eff}(Q)/2M_{eff} = M_{eff}(1 - i\Gamma_{0SM}/2M_Z) \quad (15)$$

which reduces to the often used complex-mass replacement if  $\Gamma_{0SM}^2$  is dropped. In the Lorentz-invariant limit this reproduces the well-established propagator [18, 19].

Any further corrections in the numerator of the propagator are suppressed by  $\alpha_{weak}\delta_{LIV}$ , where  $\alpha_{weak}$  is the weak fine-structure constant, and are proportional to the  $Q_\mu Q_\nu$  term. In the Drell–Yan process mediated by the neutral Z boson, which we will analyze in the later sections, in the limit of massless fermions, all vector and axial currents are conserved. Terms proportional to momentum in the numerator therefore give no contribution. Consequently, the working form of the propagator is

$$D_{\mu\nu} = \frac{ig_{\mu\nu}}{Q_\lambda^2 - M_{eff}^2(1 - i\Gamma_{0SM}/2M_Z)^2} \quad (16)$$

## 5 Phenomenology in Drell–Yan Processes

The neutral current Drell–Yan process  $pp \rightarrow Z/\gamma \rightarrow \ell^+ \ell^-$  provides the cleanest probe of LIV in the weak sector. This process is carried by the neutral intermediate bosons: photon, Z boson, and Higgs, but the Higgs channel is extremely suppressed and therefore its effects are negligible. In this process, the energy carried by the Z boson is the highest possible during proton–proton collisions. Consequently, the resonance region is particularly sensitive: even a small  $\delta_{LIV}$  may induce a measurable shift in the fitted Z mass.

When two protons collide at the LHC, they are arranged so they carry the following momenta

$$P_1 = (E, P\vec{r}), \quad P_2 = (E, -P\vec{r}) \quad (17)$$

where  $\vec{r}$  is the unit vector along the collision axis and beam, which is colinear with the detector axis. The high energy of these protons allows us to neglect the proton mass, and within this accuracy we can assume that  $E = P$ . Partons inside each proton carry an  $x$  portion of the energy, with probability  $f_{q_f}(x)$ . Thus, when protons collide and the process proceeds via the neutral current, the momentum carried by the intermediate boson after parton–antiparton annihilation is:

$$Q = x_1 P_1 + x_2 P_2 = E((x_1 + x_2), (x_1 - x_2)\vec{r}) \quad (18)$$

and the cross section of the process has the form

$$\sigma_P = \sum_f \int dx_1 dx_2 f_{q_f}(x_1) f_{\bar{q}_f}(x_2) \sigma_f \quad (19)$$

with index  $f$  denoting the flavor of the partons inside the proton,  $\sigma_P$  the cross section of the proton–proton collision, and  $\sigma_f$  the parton–antiparton (quark–antiquark) annihilation cross section. The four-momentum  $Q_\mu$  is often parametrized by the invariant mass  $M$  and rapidity  $Y$ :

$$Q_\mu = M(\cosh Y, \vec{r} \sinh Y), \quad Q_\mu^2 = M^2 \quad (20)$$

Here we note that higher rapidity corresponds to higher transferred energy and 3-momentum. If we calculate the Jacobian of this transformation,

$$\frac{\partial(M^2, Y)}{\partial(x_1, x_2)} = 4E^2 \quad (21)$$

we can define the differential cross section as

$$\frac{d^2\sigma_p}{dM^2dY} = \sum_f \frac{f_{qf}(x_1)f_{\bar{q}f}(x_2)}{4E^2} \sigma_f \quad (22)$$

We will not go into the details of the direct calculation of  $\sigma_f$ ; instead, we cite it from [12]:

$$\begin{aligned} \frac{d^2\sigma_p}{dM^2dY} = \sum_f \frac{f_{qf}(x_1)f_{\bar{q}f}(x_2)}{4E^2} \sigma_{EM} &[1 + \frac{g_q g_l (M^2 - M_{eff}^2 (1 - \Gamma_{0SM}^2 / 4M_Z^2))}{2 |e_f| M^2 \sin^2 2\theta_w} R_s \\ &+ \frac{(1 + g_q^2)(1 + g_l^2)}{16 e_f^2 \sin^4 2\theta_w} R_s] \end{aligned} \quad (23)$$

where  $e_f$  is the charge of corresponding quark,  $\sigma_{EM}$  the electromagnetic cross section, and  $R_s$  resonance factor:

$$\sigma_{EM} = \frac{4\pi\alpha^2}{9M^2} e_f^2, \quad R_s = \frac{M^4}{(M^2 - M_{eff}^2 (1 - \Gamma_{0SM}^2 / 4M_Z^2))^2 + M_{eff}^4 \Gamma_{0SM}^2 / M_Z^2} \quad (24)$$

From the cross section we see that the resonance value of the invariant mass  $M_r$  is now defined as

$$M_r^2 = M_{eff}^2 (1 - \Gamma_{0SM}^2 / 4M_Z^2) \quad (25)$$

with

$$M_{eff}^2 = M_Z^2 + \delta_{LIV} M_r^2 (n_0 \cosh Y - (\vec{n} \cdot \vec{r}) \sinh Y)^2 \quad (26)$$

Thus we can write

$$M_r^2 \approx M_Z^2 (1 + \delta_{LIV} (n_0 \cosh Y - (\vec{n} \cdot \vec{r}) \sinh Y)^2) - \Gamma_{0SM}^2 / 4 \quad (27)$$

The peak value of the cross section changes in the following manner:

$$\sigma_{f \max} \approx \sigma_{f \max}^{LI} \left(1 - \frac{\delta_{LIV} (n \cdot Q_r)^2}{M_Z^2}\right) \approx \sigma_{f \max}^{LI} (1 - \delta_{LIV} (n_0 \cosh Y - (\vec{n} \cdot \vec{r}) \sinh Y)^2) \quad (28)$$

LIV effects depend strongly on the preferred direction  $n_\mu$  and on rapidity  $Y$ . The dependence on rapidity is very strong: effects that are invisible at small rapidities may become glaring at higher rapidities.

We initially postulated  $n_\mu$  to be a unit vector, but general violation patterns do not exclude the lightlike case either, nor is anything in our assumptions or derivation sensitive

to this. Therefore, we can still distinguish three different cases of LIV: timelike, spacelike, and lightlike.

$$\text{Time-like: } n_\mu = (1, \vec{0}), \quad (29)$$

$$\text{Space-like: } n_\mu = (0, \vec{n}), \quad \text{with } \vec{n}^2 = 1, \quad (30)$$

$$\text{Light-like: } n_\mu = (1, \vec{n}). \quad (31)$$

For pure timelike violation we obtain:

$$M_r^2 \approx M_Z^2(1 + \delta_{LIV} \cosh^2 Y) - \Gamma_{0SM}^2/4 \quad (32)$$

$$\sigma_{f \max} \approx \sigma_{f \max}^{LI}(1 - \delta_{LIV} \cosh^2 Y) \quad (33)$$

Here dependence on the orientation does not exist, since in the timelike case no anisotropy appears. The dependence on  $Y$  is maximally strong. For timelike violation, separate observation of high-rapidity cases should be the strategy for LIV studies. Probably this is a good idea for any LIV case. If we want to constrain  $\delta_{LIV}$  from the accuracy of  $Z$  boson mass measurement, using  $\Delta M_Z$  (Atlas value), we can estimate:

$$\delta_{LIV} \leq \frac{2\Delta M_Z}{M_Z \cosh^2 Y} \quad (34)$$

which for  $Y = 5, 6$ , offers  $10^{-8}(10^{-9})$ .

For the spacelike violation case, alongside strong rapidity dependence, anisotropy also appears. Since  $\vec{n} \cdot \vec{r} \equiv \cos \beta$ , with  $\beta$  the angle between the preferred direction and the collision axis, the result depends on Earth's orientation in space and consequently on sidereal time:

$$M_r^2 \approx M_Z^2(1 + \delta_{LIV} \sinh^2 Y \cos^2 \beta) - \Gamma_{0SM}^2/4 \quad (35)$$

$$\sigma_{f \max} \approx \sigma_{f \max}^{LI}(1 - \delta_{LIV} \sinh^2 Y \cos^2 \beta) \quad (36)$$

Unless, by unfortunate combination,  $\cos \beta$  is very small, distinct oscillations in the cross section at high rapidity should appear with sidereal time.

For the lightlike case  $n_\mu^2 = 0$ . If this case is hard to understand separately, we can at least look at it as a limiting case of timelike or spacelike violations. When  $n_0 \gg 1$ , (27) and (28) assume a lightlike form:

$$M_r^2 \approx M_Z^2(1 + \delta_{LIV} (\cosh Y - \sinh Y \cos \beta)^2) - \Gamma_{0SM}^2/4 \quad (37)$$

$$\sigma_{f \max} \approx \sigma_{f \max}^{LI}(1 - \delta_{LIV} (\cosh Y - \sinh Y \cos \beta)^2) \quad (38)$$

Similar to the spacelike violation, the lightlike case also exhibits anisotropy, though of a different character. It is different enough to be distinguished from spacelike violation. However, this case is still a kind of hybrid between timelike and spacelike violations.

The conclusion we can quickly draw here is the following: an almost exponential dependence on rapidity and modulations by sidereal time should be the main targets of this kind of LIV study. Dependence on rapidity is the more universal property, while study of sidereal-time signal modulations may be restricted by the experimental statistics.

## 6 Experimental Strategy

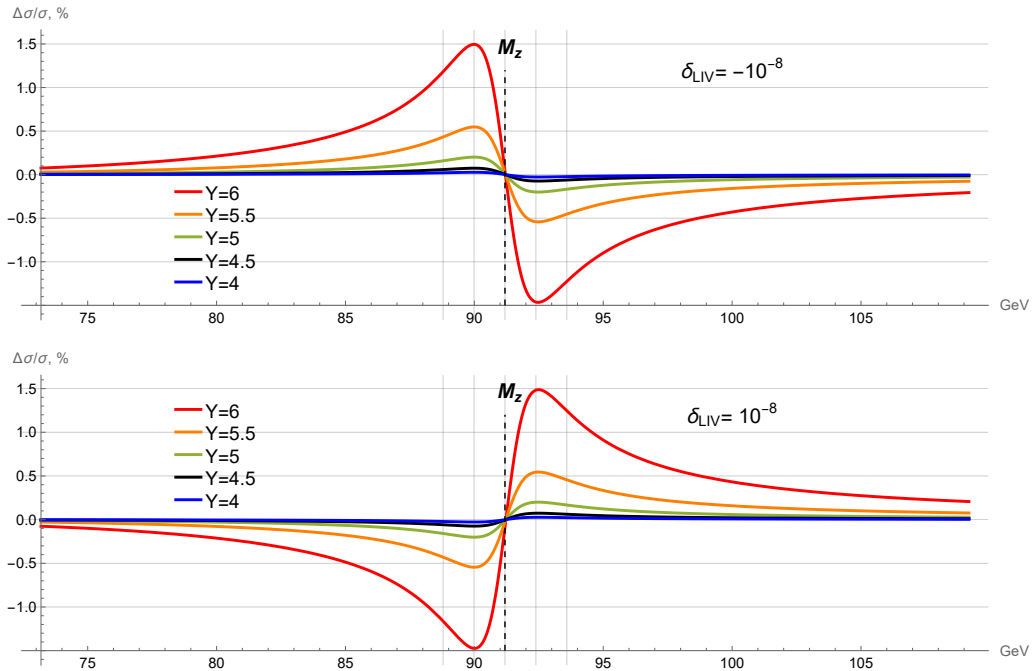
As we saw in the earlier section, the driving force behind the LIV effects comes from processes with higher rapidity. While the anisotropy appearing in the spacelike and lightlike cases will leave its mark on experimental data, large rapidities remain a prerequisite for LIV detection. If we look at the standard cross section distribution by rapidity in Drell–Yan processes [20], we can clearly identify that the vast majority of events occur at small rapidity  $Y$ , where LIV effects are virtually nonexistent. Thus, the experimentally acquired data in its vast majority will appear almost LI, with only a small fraction of events at higher  $Y$ , where LIV can in principle become pronounced.

Therefore, to increase the chance of LIV detection we need to isolate the LIV-sensitive signal by sorting the data according to rapidity and, if anisotropy is present (in the spacelike and lightlike cases), also by sidereal time. This allows event selection by transferred momentum and spatial orientation. Smaller bin sizes for event selection would naturally give a more accurate picture; however, events with higher rapidities are rare, and there is possibly a practical limit on bin size.

The pure timelike violation case should be easier to analyze, since there is no need for anisotropy searches. In each rapidity bin, statistics will be significantly better, and for the cross section near the  $Z$ -boson resonance region we will have slightly different resonance invariant masses and different peak values. Analysis of the peak's shape, size, and location should be sufficient to constrain the LIV parameters  $\delta_{LIV}$  and  $n_\mu$ .

Let us analyze the timelike violation case as a demonstration of the above-mentioned strategy. To understand the pure LIV effect, we can plot the relative difference between  $\sigma_f$  and its LI counterpart

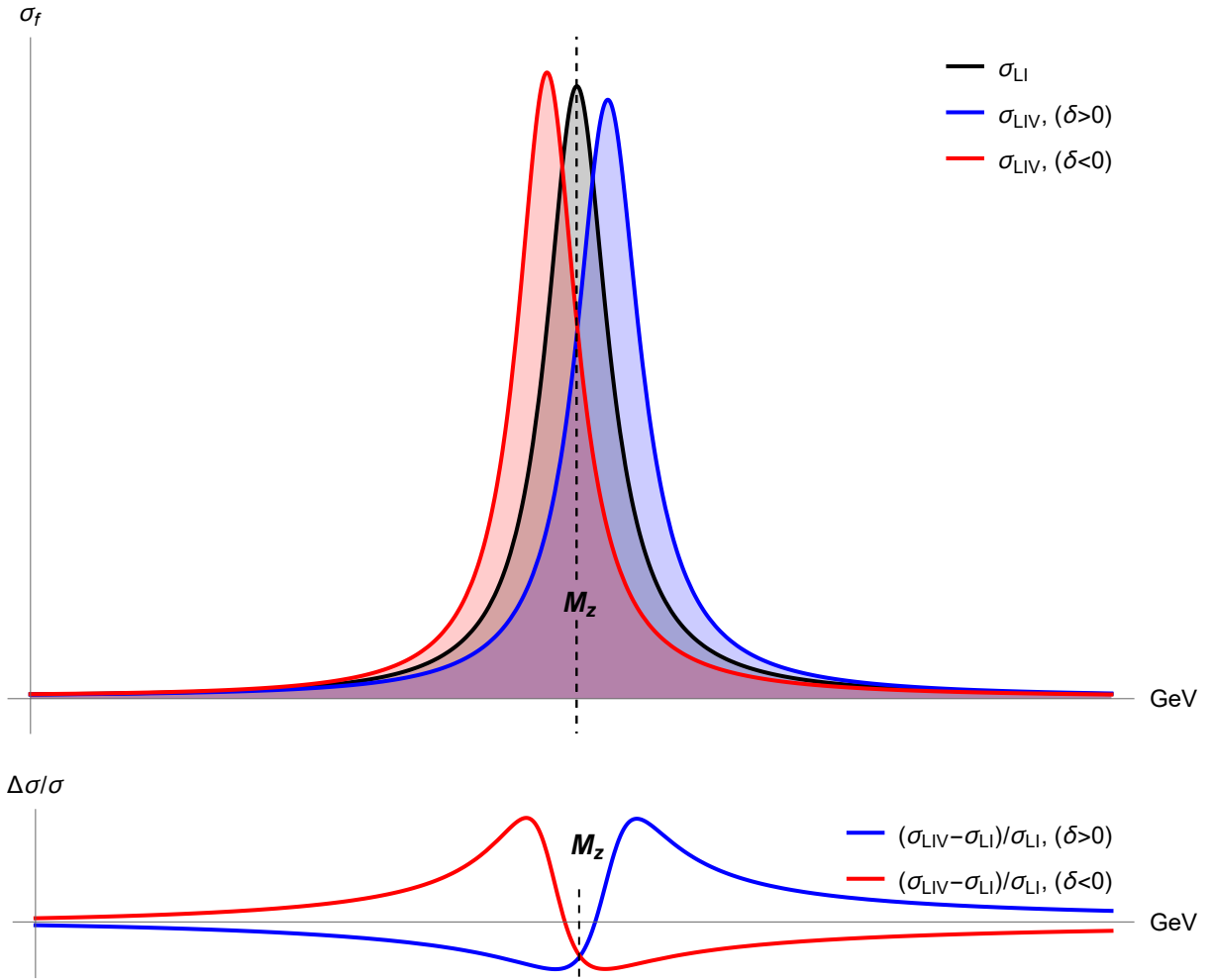
Figure 1:  $(\sigma_{LIV} - \sigma_{LI})/\sigma_{LI}$



This plot illustrates the behavior of the relative difference between the LIV and LI cross sections at the parton level, thereby isolating the LIV effect for a clearer understanding of its structure. Despite appearances, the LIV effect is not exactly zero at the resonance point. It reaches its maximum value at a point approximately 1.2 GeV away from the true mass ( $M_Z = 91.1876$  GeV).

This figure vividly illustrates how the LIV effect is activated near the resonance mass, and how the enhanced effect quickly dies out farther from the resonance, scaling as  $\delta_{LIV}$  to leading order. Inside the resonance region at  $Y = 5$ , the effect is of the order of a few tenths of a percent and increases up to about 1.5% at  $Y = 6$  for  $|\delta_{LIV}| = 10^{-8}$ . The sign of the LIV parameter  $\delta_{LIV}$  determines how the resonance peak shifts, but for both signs the approximate amplitude of the effect remains the same. This percent-level change is significant but still too subtle for the human eye to discern on the paper's scale. Therefore, next we show an exaggerated plot of the LIV and LI cross sections to better highlight the structure of the LIV effect.

Figure 2: Highly exaggerated comparison of parton's LIV and LI cross-sections.



The plot for  $Y = 8$  illustrates LIV behavior in contrast to LI. Such an explicit presentation is not feasible for  $Y = 4.5$ , where the effect amounts to only  $\sim 0.1\%$ , making it visually indistinguishable.

If LIV is present, the most likely scenario is that all data — both high rapidity (where LIV is pronounced) and low rapidity (where LIV is negligible) — will be combined together. Attempting to fit this LIV-affected cross section into an LI template still yields a result, since the effect is perturbative in nature, but with altered fitting parameters: the extracted boson mass, and to a lesser degree the decay width. To illustrate this behavior,

below we provide a table of the fitted mass shift  $\Delta M_Z$

Table 1: Absolute mass shift  $|\Delta M_Z|$  as a function of rapidity  $Y$  and the fractional composition of LI and LIV contributions of cross sections in the data.

<i>LI :</i> <i>LIV :</i>	100% 0%	90% 10%	80% 20%	70% 30%	60% 40%	50% 50%	40% 60%	30% 70%	20% 80%	10% 90%	0% 100%
Y=0.5	0eV	0.1keV	0.1keV	0.2keV	0.2keV	0.3keV	0.3keV	0.4keV	0.5keV	0.5keV	0.6keV
Y=1.0	0eV	0.1keV	0.2keV	0.3keV	0.4keV	0.5keV	0.7keV	0.8keV	0.9keV	1.0keV	1.1keV
Y=1.5	0eV	0.3keV	0.5keV	0.8keV	1.0keV	1.3keV	1.5keV	1.8keV	2.keV	2.3keV	2.5keV
Y=2.0	0eV	0.6keV	1.3keV	1.9keV	2.6keV	3.2keV	3.9keV	4.5keV	5.2keV	5.8keV	6.5keV
Y=2.5	0eV	1.7keV	3.4keV	5.1keV	6.9keV	8.6keV	10.3keV	12.keV	13.7keV	15.4keV	17.1keV
Y=3.0	0eV	4.6keV	9.2keV	13.9keV	18.5keV	23.1keV	27.7keV	32.4keV	37.keV	41.6keV	46.2keV
Y=3.5	0eV	12.5keV	25.1keV	37.6keV	50.1keV	62.6keV	75.2keV	87.7keV	100.2keV	112.7keV	125.3keV
Y=4.0	0eV	34keV	68keV	102keV	136keV	170keV	204keV	238keV	272keV	306keV	340keV
Y=4.5	0eV	92keV	185keV	277keV	370keV	462keV	0.6MeV	0.6MeV	0.7MeV	0.8MeV	0.9MeV
Y=5.0	0eV	251keV	0.5MeV	0.8MeV	1.0MeV	1.3MeV	1.5MeV	1.8MeV	2.0MeV	2.3MeV	2.5MeV
Y=5.5	0eV	0.7MeV	1.4MeV	2.0MeV	2.7MeV	3.4MeV	4.1MeV	4.8MeV	5.5MeV	6.1MeV	6.8MeV
Y=6.0	0eV	1.9MeV	3.7MeV	5.6MeV	7.4MeV	9.3MeV	11.1MeV	13.0MeV	14.8MeV	16.7MeV	18.6MeV
Y=6.5	0eV	5MeV	10MeV	15MeV	20MeV	25MeV	30MeV	35MeV	40MeV	45MeV	51MeV
Y=7.0	0eV	14MeV	27MeV	41MeV	55MeV	69MeV	82MeV	96MeV	110MeV	124MeV	137MeV

This table shows how the resonance mass shifts from the true mass value when an LIV-contaminated cross section is reconstructed as an LI Standard Model fit. The greater the contamination by LIV effects—which corresponds to events at higher rapidities—the larger the mass shift. Although real data would consist of a distribution of events across all possible rapidities, this simplified picture still serves as a clear demonstration. Depending on the event selection process, a different pattern may emerge. In particular, selecting only higher-rapidity events would yield a stronger LIV signal in the form of a mass shift. The sign of  $\delta_{LIV}$  determines whether the resonance mass is overestimated ( $\delta_{LIV} > 0$ ) or underestimated ( $\delta_{LIV} < 0$ ), but the difference in both cases remains within the displayed accuracy. For this reason, we combine both cases into a single chart.

In the table we see a numerical confirmation of our qualitative expectations. The low-rapidity cases contain virtually no LIV. If the data is a mixture of 90% LI and 10% LIV events at  $Y = 5$ , the total effect is diluted to  $|\Delta M_Z| \approx 0.25$  MeV. By contrast, if 100% of  $Y = 5$  data is analyzed, then  $|\Delta M_Z| \approx 2.5$  MeV noticeably larger than the quoted experimental uncertainty of 2.1 MeV and therefore impossible to accommodate within the declared accuracy. Clearly, for  $Y = 6$  LIV would be even easier to detect, if accelerators could access such high rapidity regimes.

This table is a kind of proxy intended to mimic the realistic effect of PDFs. Even in this simplified approximation, the nature of the LIV effect is very descriptive. Exact calculations using PDFs, or including lower-order processes, cannot alter the general behavior, though they would certainly provide a more quantitatively accurate picture.

## 7 Discussion: Z vs W Bosons

We discussed in detail the case of the Z boson because of its narrow width and clean leptonic channels, properties that make analysis of experimental data and the chance of discovering possible LIV effects more realistic. We understand that the modified dispersion relation affects the resonance region shape in a prominent way, and the effect is more pronounced at higher rapidities. The sign of the LIV parameter determines whether the shift in resonance mass is negative or positive; however, the absolute value of the shift remains approximately the same. Since in all data the pronounced LIV effect will appear only in a small fraction of events, the total divergence of the fitted parameters from

the Lorentz-invariant ones will be less noticeable. This warrants dedicated screening of high-rapidity cases in a separate analysis. In the case of anisotropy, separate binning by sidereal time will be necessary to understand the nature of the effect, although here we may encounter the practical limit imposed by insufficient statistics.

While everything said above holds, we must keep in mind that the Z boson is routinely used for calibration at hadron accelerators (LHC and CDF). This raises the question of whether such a procedure could bias against potential LIV effects, and we are not equipped to answer this question yet.

The Z boson looks like an ideal candidate for such a study in a certain sense, but everything said about the Z boson can in principle be generalized to charged W bosons as well. Interestingly, recent tensions between Tevatron and LHC measurements of  $M_W$ , resulting in a discrepancy of about 65 MeV [21], are qualitatively in line with the LIV behavior for negative  $\delta_{LIV}$ . It is yet unclear whether this discrepancy originates from experimental issues, and it is unlikely that the matter will be resolved soon. Nevertheless, if there is even partial merit to this interpretation, it would warrant serious exploration of LIV in resonance mass measurements.

Taken together, the Z and W boson cases highlight how collider observables provide a unique and complementary window on LIV, one that cannot be accessed through astrophysical probes alone. This motivates the broader conclusions we now turn to.

## 8 Conclusions and Outlook

In this work we have explored how Lorentz invariance violation (LIV) can manifest in the weak sector through modifications of the Z-boson dispersion relation. Starting from a simple but physically motivated Lagrangian deformation, we showed how only a restricted class of operators leads to observable effects, with gauge invariance necessarily compromised to ensure physical LIV. The resulting modifications impact both the propagator and resonance properties of the Z boson in a calculable way.

The Drell–Yan process provides an especially clean testing ground, as the resonance region of the Z boson is both experimentally well measured and theoretically under control. We demonstrated that LIV effects scale almost exponentially with rapidity and, in anisotropic cases, can introduce sidereal modulations. This motivates targeted analyses that separate events by rapidity and, where relevant, by sidereal time. While the majority of experimental data originates at small rapidities where LIV effects are negligible, the high-rapidity bins—though rarer—carry the dominant sensitivity. Our analysis indicates that percent-level modifications of the cross section are possible for  $|\delta_{LIV}|$  around  $10^{-8}$ , leading to effective shifts in the fitted Z-boson mass that can exceed current experimental uncertainties.

The timelike violation case offers the clearest starting point, as it avoids anisotropy and maximizes rapidity dependence, but the spacelike and lightlike scenarios remain equally important for a comprehensive picture. Our proxy estimates further show that even after dilution by parton distribution effects, the characteristic signatures of LIV remain robust.

Beyond the Z boson, similar reasoning extends to W bosons. Recent discrepancies in W-mass measurements may be qualitatively consistent with negative  $\delta_{LIV}$ , although firm conclusions require further scrutiny. Taken together, the Z and W bosons constitute an essentially unexplored sector for LIV searches, one that cannot be constrained

astrophysically and is uniquely accessible to collider experiments.

In outlook, we emphasize several directions:

1. Dedicated experimental analyses that implement binning in rapidity and, where applicable, sidereal time.

2. Extension of the study to W bosons, especially in light of current experimental tensions.

Altogether, collider studies of unstable bosons provide sensitivity to LIV possibly up the  $10^{-9}$  level, competitive with astrophysical bounds but in a complementary sector. Pursuing this line of research could therefore open a new experimental window on fundamental physics beyond the Standard Model.

## Acknowledgments

We thank Jon Chkareuli and the participants of the 25th Workshop ‘What Comes Beyond the Standard Models?’ (6–17 July, Bled, Slovenia) for valuable and fruitful discussions, and the organizers for providing a productive working environment. This work was supported by SRNSF (grant STEM-22-2604).

## References

- [1] V.A. Kostelecký, S. Samuel. Spontaneous breaking of Lorentz symmetry in string theory. *Phys. Rev. D* 39, 683 (1989). <https://doi.org/10.1103/PhysRevD.39.683>
- P. Kraus, E.T. Tomboulis. Photons and Gravitons as Goldstone Bosons, and the Cosmological Constant. *Phys.Rev. D*66 (2002) 045015.  
<https://doi.org/10.48550/arXiv.hep-th/0203221>
- R. Bluhm, A. Kostelecký. Spontaneous Lorentz Violation, Nambu-Goldstone Modes, and Gravity. *Phys.Rev.D*71:065008,2005. <https://doi.org/10.48550/arXiv.hep-th/0412320>
- J.L. Chkareuli, Z.R. Kepuladze. Massless and Massive Vector Goldstone Bosons in Nonlinear Quantum Electrodynamics. Contribution to: 14th International Seminar on High Energy Physics: Quarks 2006. <https://doi.org/10.48550/arXiv.hep-th/0610277>
- J.L. Chkareuli, J.G. Jejelava. Spontaneous Lorentz Violation: Non-Abelian Gauge Fields as Pseudo-Goldstone Vector Bosons. *Phys.Lett.B*659:754-760,2008. <https://doi.org/10.48550/arXiv.0704.0553>
- J.L. Chkareuli, C.D. Froggatt, H.B. Nielsen. Spontaneously Generated Tensor Field Gravity. *Nuclear Physics B*, V. 848, I. 3. <https://doi.org/10.48550/arXiv.1102.5440>
- J.L. Chkareuli, J.G. Jejelava, G. Tatishvili. Graviton as a Goldstone boson: Nonlinear Sigma Model for Tensor Field Gravity. *Phys.Lett.B*696:124-130,2011. <https://doi.org/10.48550/arXiv.1008.3707>
- J.L. Chkareuli, J. Jejelava, Z. Kepuladze. Lorentzian Goldstone modes shared among photons and gravitons. *Eur.Phys.J.C* 78 (2018) 2, 156. <https://doi.org/10.48550/arXiv.1709.02736>

J.L. Chkareuli, Z. Kepuladze. Gauge Symmetries Emerging from Extra Dimensions. Phys.Rev.D 94 (2016) 6, 065013. <https://doi.org/10.48550/arXiv.1607.05919>

[2] P. Horava. Quantum Gravity at a Lifshitz Point. Phys.Rev.D79:084008,2009. <https://doi.org/10.48550/arXiv.0901.3775>

[3] K.Greisen. End to the Cosmic-Ray Spectrum? Phys. Rev. Lett. 16, (1966) 748. <https://doi.org/10.1103/PhysRevLett.16.748>  
G.T. Zatsepin and V.A. Kuz'min. Upper limit of the spectrum of cosmic rays. JETP Lett. 41 (1966) 78.

[4] AGASA Collab. (M. Takeda et al.). Extension of the Cosmic-Ray Energy Spectrum beyond the Predicted Greisen-Zatsepin-Kuz'min Cutoff. Phys.Rev.Lett. 81 (1998) 1163-1166. <https://doi.org/10.48550/arXiv.astro-ph/9807193>  
AGASA Collab. (M. Takeda et al.). Energy determination in the Akeno Giant Air Shower Array experiment. Astropart.Phys. 19 (2003) 447-462. <https://doi.org/10.48550/arXiv.astro-ph/0209422>

[5] The Pierre Auger Collaboration. Features of the energy spectrum of cosmic rays above  $2.5 \times 10^{18}$  eV using the Pierre Auger Observatory. Phys. Rev. Lett. 125, 121106 (2020). <https://doi.org/10.48550/arXiv.2008.06488>  
The Pierre Auger Collaboration. Measurement of the cosmic-ray energy spectrum above  $2.5 \times 10^{18}$  eV using the Pierre Auger Observatory. Phys. Rev. D 102, 062005 (2020). <https://doi.org/10.48550/arXiv.2008.06486>  
The Pierre Auger Collaboration. The energy spectrum of cosmic rays beyond the turn-down around  $10^{17}$  eV as measured with the surface detector of the Pierre Auger Observatory. Eur. Phys. J. C (2021) 81:966. <https://doi.org/10.48550/arXiv.2109.13400>

[6] A. Giannetti, S. Marciano, D. Meloni. Exploring New Physics with Deep Underground Neutrino Experiment High-Energy Flux: The Case of Lorentz Invariance Violation, Large Extra Dimensions and Long-Range Forces. Universe 10 (2024) 9, 357. <https://doi.org/10.48550/arXiv.2407.17247>  
K. Hirata et al. [Kamiokande-II Collaboration], Phys. Rev. Lett. 58 (1987) 1490.

[7] S. Coleman, S. L. Glashow. High-Energy Tests of Lorentz Invariance. Phys.Rev.D59:116008,1999. <https://doi.org/10.48550/arXiv.hep-ph/9812418>

[8] A. Kostelecky, N. Russell. Data Tables for Lorentz and CPT Violation. Rev.Mod.Phys. 83: 11 (2011). <https://doi.org/10.48550/arXiv.0801.0287>

[9] B. Altschul. Laboratory Bounds on Electron Lorentz Violation. Phys. Rev. D 82, 016002 (2010). <https://doi.org/10.48550/arXiv.1005.2994>

[10] O. Gagnon, G.D. Moore. Limits on Lorentz violation from the highest energy cosmic rays. Phys.Rev. D70 (2004) 065002. <https://doi.org/10.48550/arXiv.hep-ph/0404196>  
Floyd W. Stecker. Constraining Superluminal Electron and Neutrino Velocities using the 2010 Crab Nebula Flare and the IceCube PeV Neutrino Events. Astroparticle Physics 56 (2014) 16. <https://doi.org/10.48550/arXiv.1306.6095>

F. Duenkel, M. Niechciol, M. Risse. Photon decay in UHE air showers: stringent bound on Lorentz violation. *Phys. Rev. D* 104, 015010 (2021). <https://doi.org/10.48550/arXiv.2106.01012>

[11] Z. Kepuladze. Lorentz Violation: Loop-Induced Effects in QED and Observational Constraints. <https://doi.org/10.48550/arXiv.2504.15608>

[12] J. Jejelava, Z. Kepuladze. Probing Lorentz Invariance Violation in Z Boson Mass Measurements at High-Energy Colliders. <https://doi.org/10.48550/arXiv.2504.11248>

[13] CMS Collaboration. Searches for violation of Lorentz invariance in top quark pair production using dilepton events in 13TeV proton-proton collisions. *Phys. Lett. B* 857 (2024) 138979. <https://doi.org/10.48550/arXiv.2405.14757>

[14] E. Lunghi, N. Sherrill, A. Szczepaniak, A. Vieira. Quark-sector Lorentz violation in Z-boson production. *JHEP* 07 (2024) 167 (erratum). <https://doi.org/10.48550/arXiv.2011.02632>

[15] J.L. Chkareuli, Z. Kepuladze. Standard model with partial gauge invariance. *Eur. Phys. J. C* 72, 1954 (2012). <https://doi.org/10.1140/epjc/s10052-012-1954-9>

[16] ALEPH, DELPHI, L3, OPAL and SLD Collaborations, LEP EW Working Group and SLD EW and Heavy Flavour Groups: S. Schael et al. Precision Electroweak Measurements on the Z Resonance. *Phys.Rept.* 427:257-454, 2006. <https://doi.org/10.48550/arXiv.hep-ex/0509008>

[17] J.L. Chkareuli, C.D. Froggatt, H.B. Nielsen. Deriving Gauge Symmetry and Spontaneous Lorentz Violation. *Nucl.Phys.B* 821:65-73,2009. <https://doi.org/10.48550/arXiv.hep-th/0610186>  
 J.L. Chkareuli, C.D. Froggatt, H.B. Nielsen. Lorentz Invariance and Origin of Symmetries. *Phys. Rev. Lett.* 87 (2001) 091601. DOI: <https://doi.org/10.1103/PhysRevLett.87.091601>  
 J.L. Chkareuli, C.D. Froggatt, H.B. Nielsen. Spontaneously generated gauge invariance. *Nucl. Phys. B* 609 (2001) 46. [https://doi.org/10.1016/S0550-3213\(01\)00283-8](https://doi.org/10.1016/S0550-3213(01)00283-8)

[18] S. Willenbrock. Mass and width of an unstable particle. *Eur.Phys.J.Plus* 139 (2024) 6, 523. <https://doi.org/10.48550/arXiv.2203.11056>.

[19] W. Greiner, B. Müller. *Gauge Theory of Weak Interactions* (fourth edition). Springer-Verlag Berlin Heidelberg, 2009.

[20] P. Banerjee, G. Das, P.K. Dhani, V. Ravindran. Threshold resummation of the rapidity distribution for Drell-Yan production at NNLO+NNLL. *Phys. Rev. D* 98, 054018 (2018). <https://doi.org/10.48550/arXiv.1805.01186>

[21] C. Hays [CDF], High precision measurement of the W-boson mass with the CDF II detector, PoS **ICHEP2022**, 898 (2022) doi:10.22323/1.414.0898  
 [CMS], Measurement of the W boson mass in proton-proton collisions at  $\sqrt{s} = 13$  TeV, CMS-PAS-SMP-23-002.  
 ATLAS Collaboration, Improved W boson Mass Measurement using 7 TeV Proton-Proton Collisions with the ATLAS Detector, ATLAS-CONF-2023-004, CERN, Geneva, 2023.